文章编号:0253-4339(XXXX)XX-0001-09
doi:10.12465/issn.0253-4339.20260821003

压电泵驱栅栏针肋壁微通道热沉流动传热性能研究

常 瑞[1] 黄永平[1] 周京京[2] 刘向东[3] 张程宾[1]

(1 东南大学能源与环境学院 南京 211189; 2 常州威图流体科技有限公司 常州 213161;
3 扬州大学电气与能源动力工程学院 扬州 225127)

摘 要 本文设计了一种压电泵驱栅栏针肋壁微通道热沉,采用数值模拟研究热沉内的流动传热特性并开展实验验证,揭示了栅栏针肋壁的强化传热机理,分析了壁面肋间距、占比及布置区域对热沉传热性能的影响。结果表明:相较于平直连续壁面的微通道热沉,间距为0.2 mm的针肋壁可以在增强流体扰动的同时扩大流固接触面积,并降低微通道的黏性摩阻,从而使热沉热阻R降低4.31%,平均努塞尔数$\overline{Nu}$提升6.26%,热性能系数TPF提高6.45%;肋间距增加至1.0 mm时,相比0.2 mm工况,热阻R进一步降低1.01%,TPF提高13.95%;在0.6 mm肋间距下,将热源区栅栏针肋壁结构占比由4.19%增至10.68%,R降低2.14%,TPF提高5.19%;而将针肋壁结构进一步拓展至非热源覆盖区(占比由10.68%增至18.15%),R仅降低0.62%,TPF仅提高1%,说明在热源区布置栅栏针肋壁结构是提升热沉传热性能的优选方案,向非热源区域扩展该结构的强化收益较低。

关键词 压电微泵;栅栏针肋壁;微通道热沉;强化传热
中图分类号:TK124;TB61+1 **文献标识码**:A

Study on Flow and Heat Transfer Performance of Piezoelectric Pump-Driven Microchannel Heat Sink with Fence Pin-Fin Walls

Chang Rui[1] Huang Yongping[1] Zhou Jingjing[2] Liu Xiangdong[3] Zhang Chengbin[1]

(1. School of Energy and Environment, Southeast University, Nanjing 211189, China; 2. Changzhou VITO Fluid Technology Co., Ltd., Changzhou 213161, China; 3. College of Electrical, Energy and power Engineering, Yangzhou University, Yangzhou 225127, China)

Abstract

Objective With the rapid increase in the integration level of microsystems, electronic components are continuously developing toward miniaturization, integration and high power, which renders high heat flux density heat dissipation a critical bottleneck restricting the development of high-end electronic devices. Piezoelectric micropumps are regarded as an ideal candidate for lightweight and thin heat dissipation systems owing to their high integration, high power-to-weight ratio and excellent controllability. In this paper, a microchannel heat sink with fence pin-fin walls driven by a piezoelectric pump is proposed. To evaluate the fluid flow and heat dissipation within the heat sink, a three-dimensional numerical modeling was performed, followed by experimental validations. The heat transfer enhancement mechanism of fence pin-fin walls is revealed, and the effects of fin spacing, area fraction and layout region of fence pin-fin walls on the thermal performance of the heat sink are analyzed.

Methods In this study, numerical simulations of the microchannel heat sink are performed using Fluent software, where a no-slip coupled boundary condition is applied to the fluid-solid interface, mixed boundary conditions are assigned to the top and bottom surfaces of the heat sink, and no-slip adiabatic boundary conditions are adopted for the remaining walls. Grid independence verification is conducted, and the total number of meshes is determined to be approximately 7.56 million. With the Reynolds number of the working fluid ranging from 35 ~ 40, the laminar model is adopted for numerical calculation, and the convergence residual criterion is set to 10^{-8}. Furthermore, experimental tests are implemented to validate the accuracy and reliability of the established numerical model.

收稿日期:2026-08-21;**修回日期**:2026-09-07;**录用日期**:2026-09-15 **责任编辑**:邵月月
基金项目:国家自然科学基金(U2441280)资助项目。(The project was supported by the National Natural Science Foundation of China (No. U2441280).)

移动阅读

Results and Discussions Numerical results reveal the heat transfer enhancement mechanism of the fence pin-fin walls structure, and clarify the effects of fence pin-fin walls spacing, area fraction and layout region on the thermal performance of microchannel heat sinks. Compared with conventional microchannels with smooth continuous wall, the fence pin-fin walls heat sink with a fin spacing of 0.2 mm reduces pressure drop by 18.87 Pa and increases flow rate by 1.03 mL/h. Such improvements decrease the thermal resistance R by 4.31% and raise the TPF (Thermal performance factor) by 6.45%, indicating that the proposed structure synergistically strengthens flow disturbance and enlarges the heat transfer area. When the fin spacing increases to 1.0 mm, the average Nusselt number $\overline{Nu}$ and TPF increase by 13.66% and 13.95%, respectively, while R decreases by 1.01%, compared with the 0.2 mm spacing case. Although the convective heat transfer area declines by 3.03% due to the reduced fin number, the average heat transfer coefficient $\overline{h}$ increases by 13.66%, effectively improving the overall thermal performance. The enhanced convective capacity fully compensates for the performance loss caused by the reduced heat transfer area. At a fixed fin spacing of 0.6 mm, increasing the fence pin-fin walls area fraction from 4.19% to 18.15% reduces thermal resistance stepwise and improves $\overline{Nu}$ and TPF. Furthermore, the fence pin-fin walls arranged in the heat source coverage region ($e_1 \sim e_3$) play a dominate role in heat transfer enhancement and thermal resistance reduction, whereas extending this structure to the non-heat source region ($e_4 \sim e_6$) yields lower enhancement benefits.

Conclusions Simulation results indicate that the microchannel heat sink with fence pin-fin walls achieves superior overall thermal performance compared with the smooth continuous wall microchannel heat sink. Appropriately enlarging pin-fin spacing strengthens the convective heat transfer inside channels, and such performance gain can offset the adverse effect arising from the reduction of heat transfer area. Within limited space, the fence pin-fin walls should be preferentially arranged in the core heat source region to fully utilize their advantages in reducing thermal resistance. According to the conclusions of this work, fence pin-fin walls with specific spacing are recommended to replace traditional smooth continuous walls in piezoelectric micropump-driven microchannels under low Reynolds number conditions. Deploying fence pin-fin walls structures preferentially in the heat source coverage region can yield better overall heat transfer performance.

Keywords piezoelectric micropump; fence pin-fin walls; microchannel heat sink; enhanced heat transfer

随着微系统集成度的飞速提升,电子元件向着小型化、集成化和高功率方向演进,高热流密度散热成为高端电子元件研发的关键瓶颈[1-2]。泵驱微通道液冷回路系统凭借传热系数高、结构紧凑、易于集成等优势,在航空航天和微电子封装等领域展现出巨大应用潜力[3-5],已成为未来高热流密度冷却散热技术的重点研究方向之一。

然而,传统泵驱微通道液冷回路系统多采用常规旋片泵,该泵体积与自重较大,难以满足便携式电子信息设备、空天小载荷装备等应用需求[6]。为此,研究者开发了多种集成化微驱动泵源,包括电磁、形变及压电驱动等[7-8]。压电微泵因其高集成性、高功重比及出色的可控性,成为轻薄化散热系统的理想选择。目前,关于压电泵驱微通道液冷的研究已取得一定进展。Tang Yong等[9]研制了一种集成压电微泵的散热器,分析了频率对散热性能的影响,加热功率为80 W时,壁面温升为47.3 ℃。Fan Yiwen等[10]将射流冲击冷却与压电微泵结合。当热流密度为91.5 W/cm^{2}时,传热系数为20.6 kW/(m^2·K)。He Lipeng等[11]通过多腔压电泵联用,进一步提升了系统降温效果。

压电泵驱动微通道液冷技术在轻薄化散热场景中具备良好应用潜力,但受限于本征驱动压头较小,微通道内工质流动常处于低雷诺数(Re)稳定层流状态。因此,如何在压电泵有限驱动能力下实现微通道传热性能强化,已成为该技术研发的重难点。目前,研究者多采用无外源被动式强化方式,通过扰流板、肋/翅片、壁面凹腔等以增强传热性能。Chai Lei等[12]研究了侧壁扇形肋条微通道内层流换热的传热流动特性,偏置扇形肋条微通道的平均努塞尔数(Nu)最高提升103%。Li Chunquan等[13]对带有肋条和针鳍的嵌入式微通道散热器展开传热性能分析,当Re=458时,传热性能提升63.91%,压降增加10.24%。Wu Andong等[14]对扇形腔圆肋微通道散热器进行数值研究,虽然该结构显著增加压降,但促进流体内部形成涡流,使平均温度降低20 ℃。

综上所述,现有微通道被动强化传热研究多聚焦于各类形状复杂的肋、槽及组合,虽能提升换热效率,但通道内部压降损失大幅增加。对于驱动能力受限的压电微泵而言,过高的阻力会限制循环流量,进而削弱整体散热效率。因此,针对上述不足,本文提出一种栅栏针肋壁结构。该结构在降低流动阻力的前提下,利用针肋增强微通道内扰流的同时,提升对流传热面积,从而提高传热效率。为揭示压电泵驱栅栏针肋壁微通道的热工水力特性,本研究采用了数值模拟与实验验证的策略,并与平直连续壁面微通道的散热性能进行了对比。研究了栅栏针肋壁间距及体积占比对压电泵驱微通道热沉性能的影

响,为高性能集成化散热系统提供参考。

1 计算模型

1.1 物理模型

压电泵驱微通道热沉整体结构如图1(a)所示。热沉整体尺寸为214 mm(L)×87 mm(W_0)×330 μm(h_1)。上下层聚对苯二甲酸乙二醇酯(polyethylene terephthalate,PET)厚度均为40 μm,流体域厚度为250 μm。热源尺寸为34 mm(a)×34 mm(a)。主通道宽度为2.38 mm(w_1),通道间壁宽为0.5 mm(w_2)。图1(e)所示为栅栏针肋壁间距S_5=0.6 mm时(不同栅栏针肋壁间距S_j的具体数值见表2,i取值为1~9),针肋面积占比E_6=18.15%的结构示意图(E_j的定义见式1,j取值为1~6)。

表1所示为压电泵驱微通道热沉具体结构参数。表2所示为不同栅栏针肋壁间距的具体取值,表3所示为S_5=0.6 mm时,不同栅栏针肋壁结构的体积占平直连续壁面所有侧壁体积的百分比。

E_j计算如下:

$$E_j = \frac{\sum_{k=1}^{j} e_k}{V_{\text{all}}} \times 100\%,\ (j = 1 \sim 6) \tag{1}$$

式中:V_{all}为平直连续壁面流道所有侧壁的体积之和,mm^3;$\sum_{k=1}^{j} e_k$为e_k至e_j区域所有栅栏针肋壁体积之和,mm^3。

本文针对e_1~e_6区域(e_1~e_3区域为热源覆盖区,e_4~e_6区域为非热源覆盖区)。在保持S_5=0.6 mm的前提下,依次将该区域内的平直连续壁面流道侧壁优化为栅栏针肋壁,重点研究了不同针肋壁结构体积占比及布置区域对热沉性能的影响。需要说明的是,对于起主要力学支撑作用的变径宽肋区未进行针肋化处理。此外,综合考虑压电微泵与热沉的装配定位要求与泵出口流体的导流效果,热沉进出口延长区域的平直连续流道侧壁也未进行针肋化处理。

1.2 理论建模

1.2.1 控制方程

本研究采用三维CFD方法模拟计算热沉流动与传热特性,为简化计算做如下假设:

1)流体为不可压缩定常流动;

2)忽略热沉0.33 mm厚度方向四周边壁的热损失;

3)不考虑流体黏性耗散的影响。

根据上述假设,热沉的控制方程如下。

连续性方程:

$$\nabla \cdot V = 0 \tag{2}$$

动量方程:

$$\rho_{\text{f}}(V \cdot \nabla V) = \cdot -\nabla P + \nabla(\mu_{\text{f}} \cdot \nabla V) \tag{3}$$

流体能量方程:

$$\rho_{\text{f}} C_{p,\text{f}} V \cdot \nabla T_{\text{f}} = k_{\text{f}} \nabla^2 T_{\text{f}} \tag{4}$$

固体区能量方程:

$$k_{\text{s}} \nabla^2 T_{\text{s}} = 0 \tag{5}$$

式中:V为流体速度,m/s;ρ_{f}为密度,kg/m^3;P为压力,Pa;μ_{f}为动力黏度,Pa·s;$C_{p,\text{f}}$为流体比定压热容,J/(kg·K);T_{f}、T_{s}分别为流体、固体温度,℃;k_{f}、k_{s}分别为流体、固体导热系数,W/(m·K)。

1.2.2 边界条件

微通道热沉仿真计算边界条件如下:

1)微通道入口采用质量流量入口,其具体数值为压电微泵的P–Q特性曲线与流道阻力曲线耦合点(图4);

2)热沉稳定工作时进出口温度一致;

3)出口为压力出口,表压为0;

4)加热面为恒热流边界条件,热通量为4 325.26 W/m^2;

5)热沉固体为PET,比热容、密度、导热系数分别为1 400 J/(kg·K)、2 000 kg/m^3、0.2 W/(m·K);采用去离子水为工质,热物性与温度之间的映射关系采用多项式拟合[15];

6)流体与固体接触壁面为无滑移耦合边界,其余壁面为无滑移绝热边界。

7)热沉上、下表面为混合边界条件,其自然对流传热系数分别为8.8、4.4 W/(m^2·K),表面发射率为0.45[16]。

1.2.3 数值模拟方法

采用Fluent软件对微通道热沉进行数值模拟,使用SIMPLE算法对控制体积内的速度、压力和温度进行求解。本研究中工质Re为35~40,采用层流模型进行模拟。残差值小于10^{-8}时判断连续性方程、动量及能量方程收敛[15]。

1.2.4 微通道流动传热性能参数定义及计算

在评价热沉的热力学性能时,热阻是一项关键参数,其计算如下:

$$R_{\text{th}} = \frac{T_{\text{h}} - T_{\text{c}}}{q \times A_{\text{q}}} \tag{6}$$

式中:T_{h}、T_{c}为发热面平均温度和对流传热面平均温度,℃;q为热流密度,W/m^2;A_{q}为加热面积,m^2。

热源区域平均对流传热系数为:

$$\bar{h} = \frac{qA_{\text{q}}}{A_{\text{c}}(T_{\text{c,avg}} - T_{\text{f,avg}})} \tag{7}$$

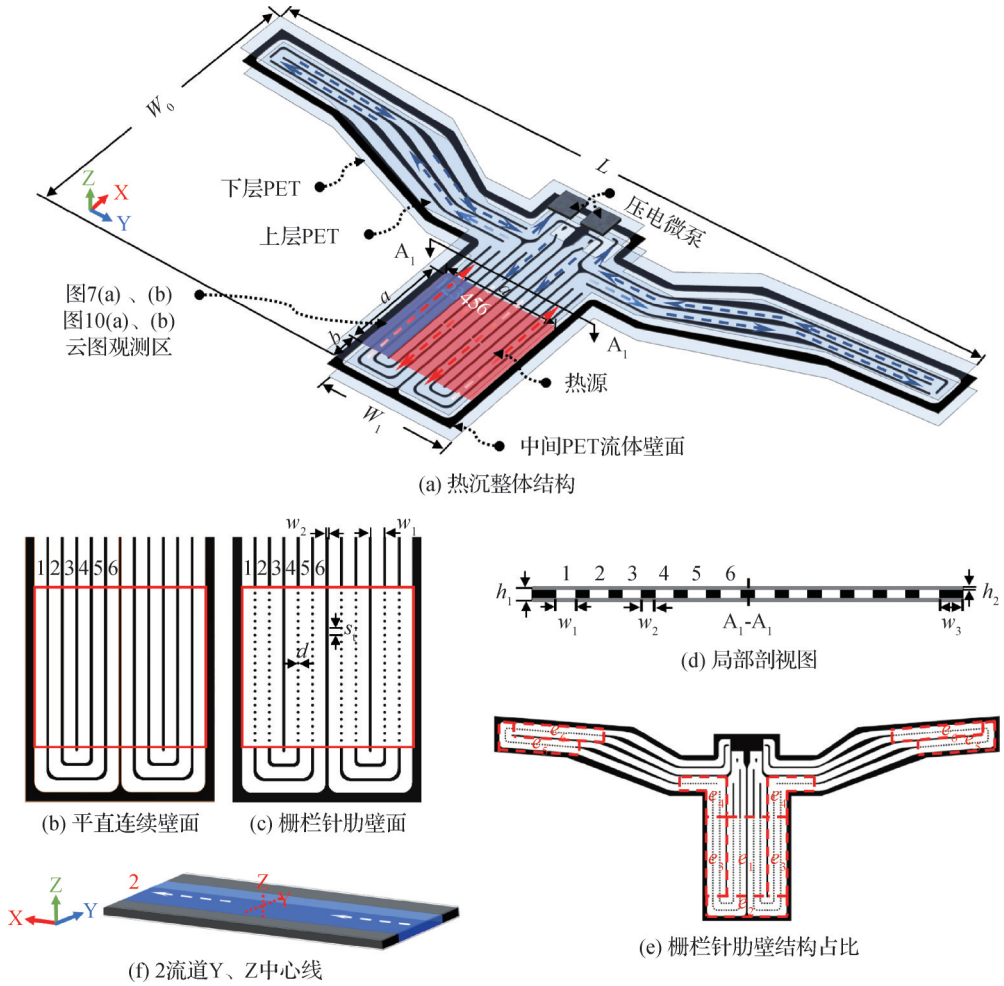


图 1 微通道热沉几何结构

Fig.1 Schematic of microchannel heat sink geometry

表 1 热沉几何参数

Tab.1 Geometric parameters of the heat sink

参数	尺寸/mm	参数	尺寸/mm
L	214.00	h_2	0.04
W_0	87.00	w_1	2.38
W_1	37.60	w_2	0.50
a	34.00	w_3	1.80
b	10.00	w_4	16.75
h_1	0.33	w_5	2.38
L	214.00	h_2	0.04
W_0	87.00	w_1	2.38

表 2 不同间距参数

Tab.2 Different spacing parameters mm

S_1	S_2	S_3	S_4	S_5	S_6	S_7	S_8	S_9
0.2	0.3	0.4	0.5	0.6	0.7	0.8	0.9	1.0

式中：A_c为对流传热面积，m²；$T_{c,avg}$、$T_{f,avg}$分别为热源处对流传热面的平均温度和冷却水体平均温度，℃。

表 3 不同栅栏针肋壁占比

Tab.3 Fraction of different fence pin-fin walls %

E_1	E_2	E_3	E_4	E_5	E_6
4.19	6.50	10.68	13.25	15.70	18.15

σ_t表征热沉表面均温[16]。采用等间距布点的方式，从入口至出口沿着流动方向等间距布置30个温度检测点。计算如下：

$$\bar{T} = \frac{1}{30}\sum_i T_i \tag{8}$$

$$\sigma_t = \sqrt{\frac{1}{15}\sum_i (T_i - \bar{T})^2} \tag{9}$$

式中：$\bar{T}$为30个温度测点的平均值，℃。

热源区域的平均努赛尔数以及微通道的水力直径计算如下：

$$\overline{Nu} = \bar{h}D_c/k_f \tag{10}$$

$$D_c = \frac{2H_cW_c}{H_c + W_c} \tag{11}$$

式中：D_c为水力直径，m；H_c、W_c分别为流道高度和宽

度，m。

微通道内摩擦因数计算如下：

$$f=\frac{D_c}{4L}\cdot\frac{\Delta P}{(1/2)\rho_f V^2} \tag{12}$$

式中：L为微通道长度，m；ΔP为压降，Pa。

为综合权衡对流传热性能与压降的影响，并判断传热强化程度，引入热性能系数（thermal performance factor，TPF）[17]，计算如下：

$$\mathrm{TPF}=\frac{\overline{Nu}/\overline{Nu_0}}{(f/f_0)^{1/3}} \tag{13}$$

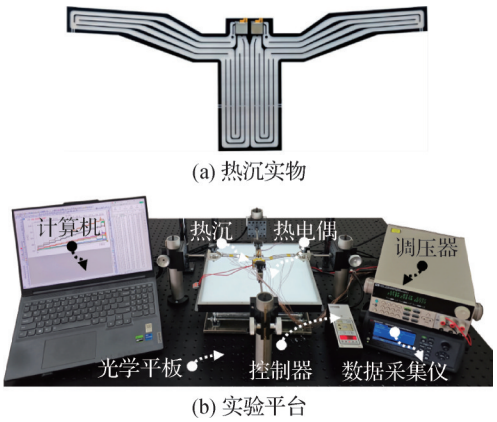
式中：$\overline{Nu_0}$、f_0分别为平直连续壁微通道热沉热源区的平均努塞尔数和摩擦因数。

1.2.5 网格独立性检验

为排除网格数量对计算求解精度的干扰，本文对模型进行网格独立性检验，并对比微通道热沉在不同网格数量下的压降ΔP及流体域最高温T_{max}的模拟值。当网格数量为757万时，ΔP与T_{max}模拟值较之前较低数量网格的相对偏差分别为0.002%和0.11%。鉴于此，为了兼顾计算资源的消耗和计算精度，网格数量至少为757万。

1.2.6 模型验证

为验证数值模型的真实可靠性，研制了如图2所示的压电泵驱微通道热沉，并搭建了性能测试平台。测试对比了不同热负荷下平直连续壁面微通道热沉热阻实测值与数值模拟值。实验数据与仿真结果在图3中展现较高的一致性，证实所构建模型的有效性。



(a) 热沉实物

(b) 实验平台

图2 热沉实物及实验平台

Fig.2 Physical heat sink and experimental platform

2 结果分析与讨论

2.1 栅栏针肋壁微通道强化散热性能分析

为了对栅栏针肋壁微通道强化传热原理进行研究，将如图1(b)所示的热源区域平直连续壁面通道作为对照组S_0，并以此为基础，通过数值模拟对比分析了其与典型栅栏针肋壁微通道热沉S_1=0.2 mm的流动传热特性，揭示栅栏针肋壁的强化传热机制。

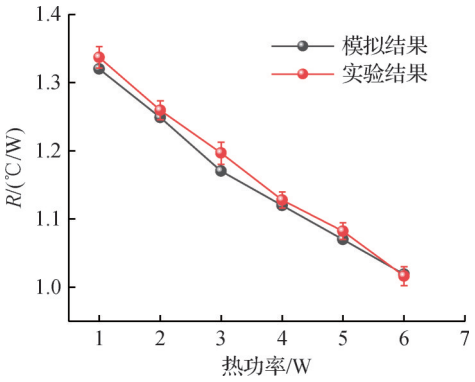


图3 模拟值与实验值

Fig.3 Simulated and experimental values

由图4可知，S_1热沉压降相较于S_0热沉压降下降18.87 Pa，流量提升了1.03 mL/h。结合图5分析可知，这主要是因为在压电泵驱动的低Re工况下，栅栏针肋结构将平直连续壁面离散化，缩减了流体与壁面的接触区域，削弱了垂直主流方向的近壁速度梯度，从而减小近壁黏性剪切力，降低微通道黏性摩擦阻力。该阻力衰减效应促使压电微泵工况点向大流量区间偏移，通道整体质量流量得以提升。

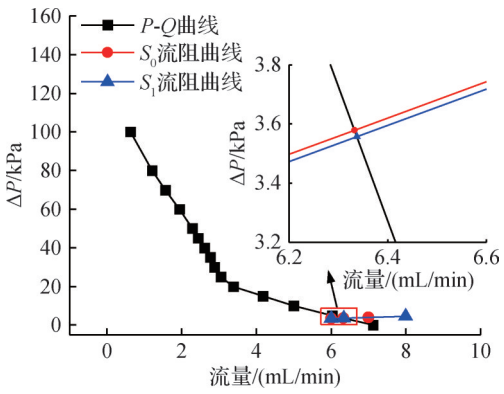


图4 压电泵*P*-*Q*曲线与流道阻力曲线交汇

Fig.4 Intersection of piezoelectric pump *P*-Q and flow resistance curve

图6所示为平直连续壁面与栅栏针肋壁热沉流动与传热性能对比。由图6(a)可知，栅栏针肋壁流道热沉的热阻相较于平直连续壁面微通道热沉降低4.31%，TPF提高6.45%，$\overline{Nu}$提升6.26%。此外，图6(b)表明，栅栏针肋壁流道热沉的A_c提升6.16%，$\overline{h}$升高6.26%。这主要因为栅栏针肋壁结构协同实现了扰流强化与换热面积提升。由上述分析可知，该结构减小了近壁面的速度梯度增强了热沉工质的循环热运输能力。

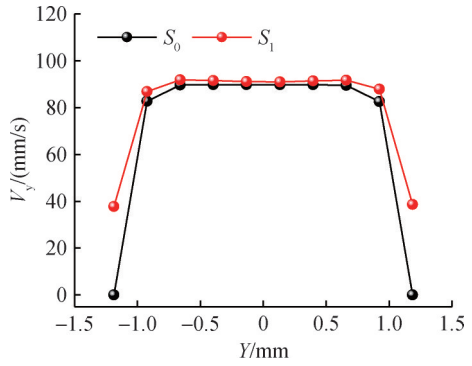


图5 2通道中心线*Y*方向速度

Fig.5 *Y*-velocity along centerline of channel 2

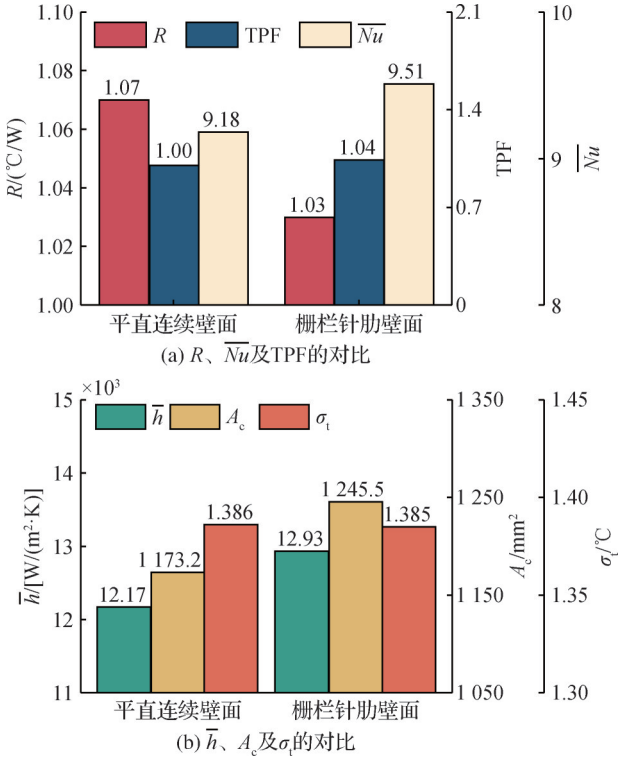


图6 平直连续壁面与栅栏针肋壁热沉流动与传热性能对比

Fig.6 Heat sink performance between smooth continuous and fence pin-fin walls

图7所示为局部热源区域热流场。由图7(a)可知,相比于S_0微通道热沉,S_1微通道热沉高温区域覆盖面积减小,但在不同流道间仍存在温度不均匀,即3通道平均温度依次大于2通道、1通道。结合图7(b)可知,虽然3通道获得了较高流速,但流体在3通道进口的基准温度显著高于1通道。较高的进口基准温度不仅对冲了高流速带来的换热增益,还缩小了流体与固体间的有效换热温差。最终使热沉热源区呈现为外侧温度低,内侧温度高的热分布特征。由图7(c)可知,S_1、S_0各通道压力均沿着流动方向逐渐降低,但S_1微通道能够有效均衡微通道内部各子流道压力,减小流道之间的压力差异。

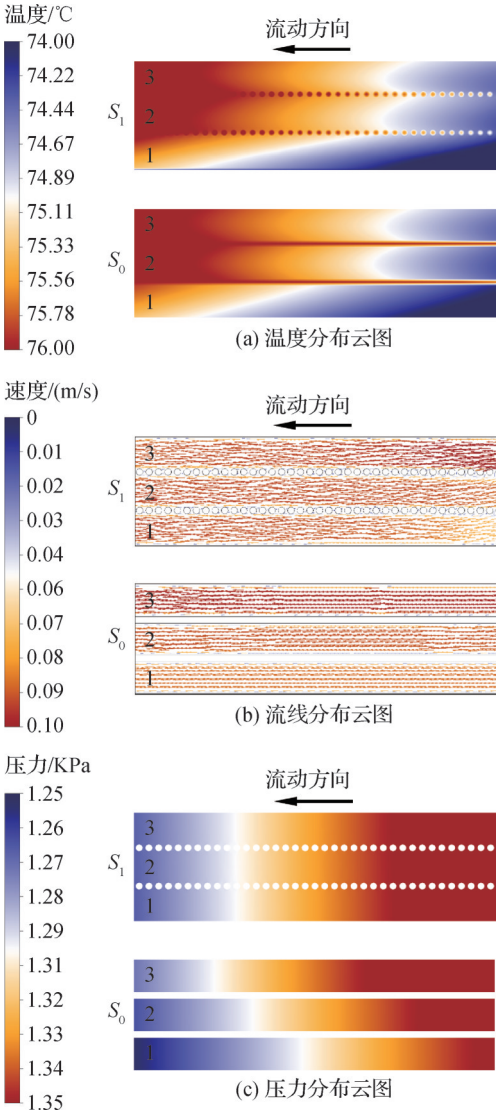


图7 局部热源区域热流场

Fig.7 Thermal and flow fields in the local heat source region

2.2 栅栏针肋壁间距对微通道性能影响

图8所示为不同栅栏针肋壁的间距S_i对热沉性能的影响。由图8(a)、(b)可知,随着肋间距升至S_9=1.0 mm时,相较于S_1=0.2 mm,$\overline{Nu}$提升13.66%,TPF提升13.95%,R降低1.01%。此时,A_c因总肋数的减小而降低3.03%,但$\overline{h}$升高13.66%,热沉整体传热性能得到一定改善。这是因为,热沉传热性能的变化主要取决于2种效应的相互竞争。一方面,间距增大导致A_c缩减;另一方面,随着间距增加,近壁面Y方向的速度梯度逐渐降低,进一步降低流阻,使得通道内部的对流传热能力提高,$\overline{h}$得到提升,补偿并超过了因对A_c衰减对传热产生的负面效应(图9)。

图10所示为不同间距局部热源区域热流场。由图10(a)可知,间距的增大进一步减少了针肋壁的局部高温热点,增加了低温区域面积。值得注意的是,

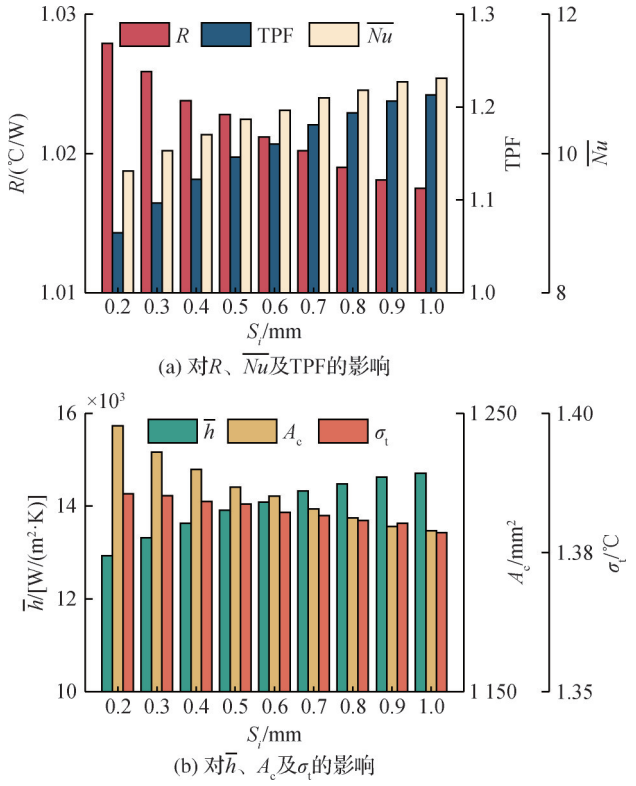


图 8 不同栅栏针肋壁的间距对热沉性能的影响

Fig.8 Effects of different fence pin-fin walls spacings on heat sink performance

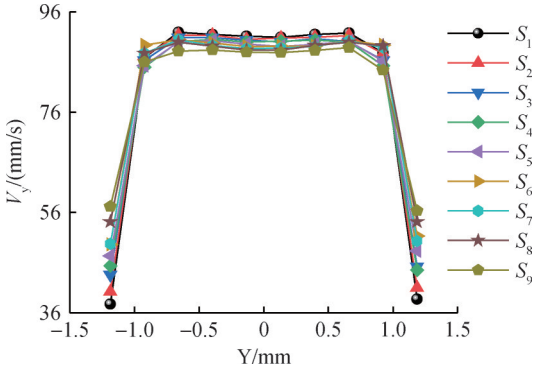


图 9 不同间距在2通道中心线 *Y* 方向的速度

Fig.9 *Y*-velocity along centerline of channel 2 for different spacings

随着针肋间距的增大，提高了通道内的质量流量，并使得不同通道间的流速更加均匀。由图 10(b)可知，相邻针肋间的扰流流速随着间距的增大而逐渐升高，不同通道间的速度差逐渐减小，内部流速逐渐趋于均匀。

2.3 栅栏针肋壁占比对热沉性能的影响

为探究不同栅栏针肋壁体积占比及布置区域对热沉传热性能的影响，在保持针肋壁间距 S_5=0.6 mm 的前提下，依次将如图 1(e)所示 e_1 ~ e_6 区域的平直连续壁面流道侧壁设置为栅栏针肋壁，由此通过数值

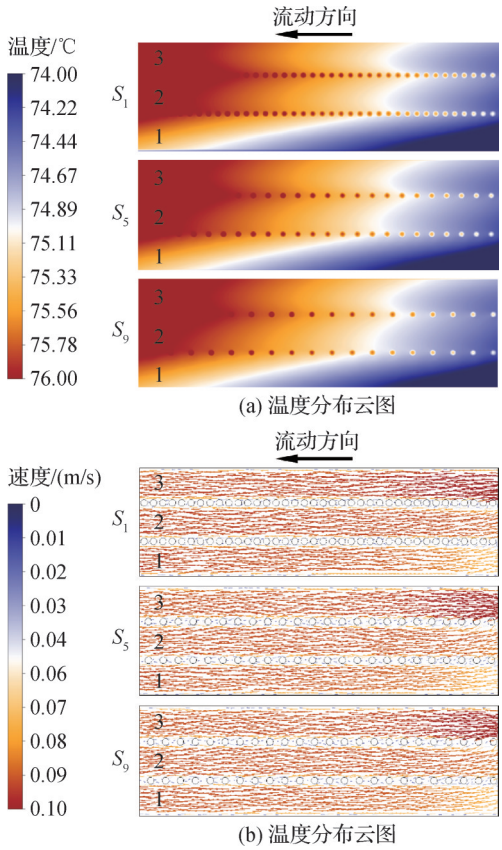


图 10 不同间距局部热源区域热流场

Fig.10 Comparison of local thermo-flow fields in the heat source region for different spacings

模拟对比分析了针肋壁体积占比 E_j(j=1 ~ 6)依次为 4.19%、6.5%、10.68%、13.25%、15.7%、18.15% 时，栅栏针肋壁微通道热沉的流动传热特性。其中，当 E_j(j=1 ~ 3)依次为 4.19%、6.5%、10.68% 时，栅栏针肋壁结构均布置于热源区 e_1 ~ e_3；E_j(j=4 ~ 6)依次为 13.25%、15.7%、18.15% 时，栅栏针肋壁结构由热源区进一步扩展至非热源区 e_4 ~ e_6。

图 11 所示为不同占比的栅栏针肋壁对热沉性能的影响。由图 11(a)可知，随着栅栏针肋壁占比从 4.19% 升至 18.15%，R 呈现出明显的下降趋势，而 $\overline{Nu}$ 和 η 逐渐上升。值得注意的是，当栅栏针肋壁结构覆盖热源核心区 e_1 ~ e_3 时，热阻 R 降低了 2.14%，TPF 提高了 5.19%。而在非热源覆盖区 e_4 ~ e_6 时，当针肋壁占比由 10.68% 增加至 18.15%，热阻 R 仅降低 0.62%，TPF 仅提高 1%。说明栅栏针肋壁优先布置于热源覆盖区更有利于发挥强化传热作用，其通过降低压降、提高流量以及强化热源区对流换热，可显著降低热源温度和整体热阻。而对于非热源区域，尽管针肋壁增加了局部换热面积，但由于基材导热能力有限且外界自然对流换热系数较低，局部温降难以向热源区传递，因此对整体热阻的改善作用较弱。

由图11(b)可知,随着栅栏针肋壁占比由4.19%升至18.15%,最高温度T_{max}由81.27 ℃降至79.77 ℃,而T_{min}略有上升,使得σ_t减小。这进一步说明,热源覆盖区$e_1 \sim e_3$的针肋壁承担着强化散热的主导作用,而向非热源$e_4 \sim e_6$区域扩展该结构的强化收益较低。

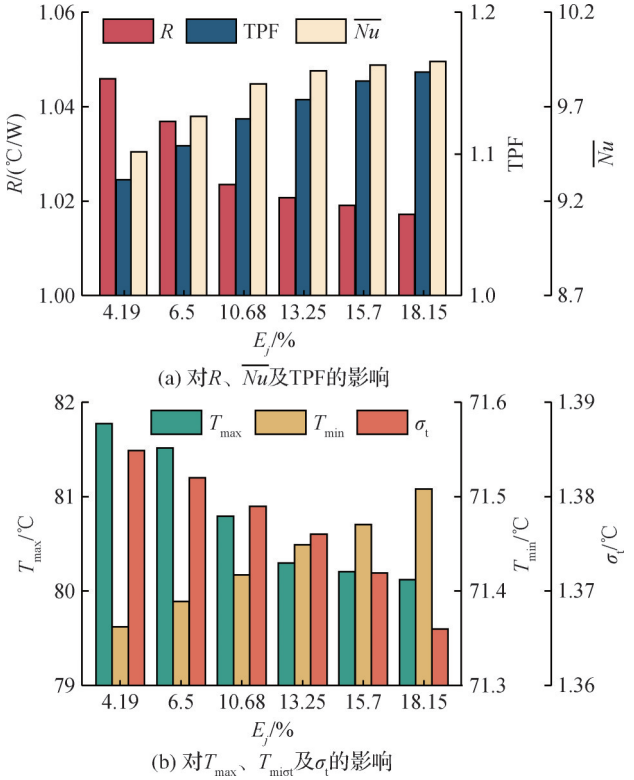


图11 不同占比的栅栏针肋壁对热沉性能的影响

Fig.11 Effect of different proportions of fence pin-fin walls on heat sink performance

3 结论

本文模拟探究了一种压电泵驱栅栏针肋壁微通道热沉的流动传热特性,与传统平直连续壁面微通道热沉进行对比,揭示了栅栏针肋壁结构的强化传热机理。探究了栅栏针肋壁间距、占比及布置区域对热沉传热性能的影响规律,得到结论如下:

1)相较于平直连续壁面微通道热沉,肋壁间距为S_1=0.2 mm的栅栏针肋壁微通道热沉压降降低18.87 Pa,流量提高1.03 mL/h。栅栏针肋壁在增强流体扰动的同时扩大了流固接触面积,削弱垂直主流方向的近壁速度梯度,从而减小近壁黏性剪切力,降低了微通道黏性摩阻。使热沉热阻R降低4.31%,TPF提高6.45%,表现出更优的综合传热性能。

2)当肋壁间距升至S_9=1.0 mm时,与S_1=0.2 mm相比,尽管对流传热面积A_c减小3.03%,但TPF提升13.95%,R降低1.01%,$\overline{h}$升高13.66%。这表明,适当增大针肋间距能够强化通道对流换热,其增益足以抵消因换热面积减小带来的不利影响。

3)在给定肋间距S_5=0.6 mm时,热源核心区$e_1 \sim e_3$的栅栏针肋壁结构占比由4.19%增至10.68%,R降低2.14%,TPF提高5.19%。而非热源覆盖区$e_4 \sim e_6$的栅栏针肋壁结构占比由10.68%增至18.15%,热阻R仅降低0.62%,TPF仅提高1%。这表明,在热源区布置栅栏针肋壁结构是提升热沉传热性能的优选方案,而向非热源$e_4 \sim e_6$区域扩展该结构的强化收益较低。

参考文献

[1] Gönül A, Okbaz A, Kayaci N, et al. Flow optimization in a microchannel with vortex generators using genetic algorithm[J]. Applied Thermal Engineering, 2022, 201: 117738.

[2] 陈超伟, 王鑫煜, 辛公明. 多孔鳍歧管微通道流动传热特性研究[J]. 制冷学报, 2022, 43(3): 62-70. (Chen Chaowei, Wang Xinyu, Xin Gongming. Flow and heat transfer characteristics in manifold microchannel with porous fins[J]. Journal of Refrigeration, 2022, 43(3): 62-70.)

[3] Deng Daxiang, Zeng Long, Sun Wei. A review on flow boiling enhancement and fabrication of enhanced microchannels of microchannel heat sinks[J]. International Journal of Heat and Mass Transfer, 2021, 175:121332.

[4] Wu Wei, Zhai Chong, Sui Zengguang, et al. Proton exchange membrane fuel cell integrated with microchannel membrane-based absorption cooling for hydrogen vehicles [J]. Renewable Energy, 2021, 178:560-573.

[5] Jiang Zhuyan, Zhang Kaihui, Du Lilong, et al. Construction of chitosan scaffolds with controllable microchannel for tissue engineering and regenerative medicine [J]. Materials Science and Engineering: C, 2021, 126: 112178.

[6] Lindh P M, Petrov I, Semken R S, et al. Direct liquid cooling in low-power electrical machines: proof-of-concept [J]. IEEE Transactions on Energy Conversion, 2016, 31 (4): 1257-1266.

[7] Tong Wenyi, Fan Desong, Yang Yue, et al. Piezoelectric micropump cooler for high-power electronic cooling [J]. International Journal of Heat and Mass Transfer, 2024, 233: 126062.

[8] Peng Yunhao, Wang Daihua, Li Xinyu, et al. Cooling chip on PCB by embedded active microchannel heat sink [J]. International Journal of Heat and Mass Transfer, 2022, 196:123251.

[9] Tang Yong, Jia Mingze, Ding Xinrui, et al. Experimental

investigation on thermal management performance of an integrated heat sink with a piezoelectric micropump[J]. Applied Thermal Engineering, 2019, 161: 114053.

[10] Fan Yiwen, Zhang Xinfeng, Xiang Linyi, et al. A compact jet array impingement cooling system driven by integrated piezoelectric micropump[J]. International Journal of Heat and Mass Transfer, 2023, 205:123905.

[11] He Lipeng, Wu Xiaoqiang, Zhang Zheng, et al. Thermal management analysis of serial-connection three-chamber piezoelectric pump[J]. Journal of Mechanical Science and Technology, 2021, 35(10): 4523-4530.

[12] Chai Lei, Xia Guo dong, Wang Hua sheng. Parametric study on thermal and hydraulic characteristics of laminar flow in microchannel heat sink with fan-shaped ribs on sidewalls - Part 1: Heat transfer[J]. International Journal of Heat and Mass Transfer, 2016, 97: 1069-1080.

[13] Li Chunquan, Li Xuebin, Huang Hongyan, et al. Hydrothermal performance analysis of microchannel heat sink with embedded module with ribs and pin-fins[J]. Applied Thermal Engineering, 2023, 225: 120167.

[14] Wu Andong, Cheng Qing, Wang Han. Research on flow and heat transfer characteristics of microchannel heat sinks with fan-shaped cavities and circular ribs [J]. International Journal of Heat and Fluid Flow, 2025, 112: 109758.

[15] 朱飞跃, 朱崎峰, 苏瑞瑞, 等. 肋槽组合式微通道流动与传热特性研究[J]. 工程热物理学报, 2023, 44(9): 2504-2513. (Zhu Feiyue, Zhu Qifeng, Su Ruirui, et al. Study on flow and heat transfer characteristics of microchannel with combined ribs and grooves[J]. Journal of Engineering Thermophysics, 2023, 44 (9): 2504-2513.)

[16] 徐晨杰, 刘向东, 周京京, 等. 压电泵驱超薄微通道热沉流动与传热特性优化的数值研究[J]. 热能动力工程, 2026, 41(4): 108-118. (Xu Chenjie, Liu Xiangdong, Zhou Jingjing, et al. Numerical study on optimization of flow and heat transfer characteristics in piezoelectric pump-driven ultra thin microchannel heat sink[J]. Journal of Engineering for Thermal Energy and Power, 2026, 41 (4): 108-118.)

[17] Zhang Yongliang, Li Min. Research on flow and heat transfer characteristics of heat transfer surface of trapezoidal duct[J]. Heat and Mass Transfer, 2020, 56 (5): 1475-1486.

通信作者简介

黄永平,男,助理研究员,东南大学能源与环境学院,13276672051,E-mail:yphuang2022@seu.edu.cn。研究方向:传热传质。

About the corresponding author

Huang Yongping, male, assistant researcher, School of Energy and Environment, Southeast University, 86-13276672051, E-mail: yphuang2022@seu.edu.cn. Research fields: heat and mass transfer.